ARRAY GEOMETRY OPTIMIZATION FOR REGION-OF-INTEREST BROADBAND BEAMFORMING

Yuval Konforti *Israel Cohen* *Baruch Berdugo*

Andrew and Erna Viterbi Faculty of Electrical and Computer Engineering
Technion – Israel Institute of Technology, Haifa 3200003, Israel
yuvalkon94@gmail.com, icohen@ee.technion.ac.il, bbaruch@technion.ac.il

ABSTRACT

Optimization of a microphone array geometry has an important impact on the beamforming performance. Though the environment settings may change in time, microphone locations are typically preserved. Thus, the selected locations are of significant importance. Moreover, if the source of interest emits a broadband signal from a location that varies in time, finding the optimal geometry becomes a challenging task. This paper introduces an efficient algorithm to find the optimal placements of microphones in a nonuniform linear array for broadband high directivity beamforming. The proposed method maintains high white noise gain (WNG) for sufficient robustness and considers several look directions in a region-of-interest (ROI) for a moving source. Compared to standard designs, our design achieves higher directivity toward any look direction in the ROI.

***Index Terms*—** Array processing, microphone array optimization, robust superdirective beamforming.

1. INTRODUCTION

Sensor array beamforming is a widely-used method for spatial filtering [1–3]. Two factors impact the performance: the array geometry and the filter coefficients. Concerning the array geometry, typical microphone arrays use simple symmetric geometries such as uniform linear arrays (ULAs), uniform circular arrays (UCAs), and uniform concentric circular arrays (UCCAs). Recently, more efforts were made to find optimal geometries for several tasks [4–12]. Such methods optimize the sensor locations, usually with a genetic algorithm [4–9] or with a greedy-based approach [10–12]. These methods may converge to an undesired local optimum, and some works consider narrowband signals only [4–6].

Several works have investigated region-based [13–21] and constant-beamwidth [22–24] beamformers directed toward a region of interest (ROI). These designs are practical when several angles of arrival are considered. Such a scenario is encountered when the source is distributed, moving, or there is some uncertainty in the source direction. Inspired by these works, we revisit the problem of array geometry optimization for region-based beamforming. A similar study was conducted in [4] but did not consider broadband signals.

This work introduces an algorithm that finds a nonuniform linear array geometry that enables high directivity beamforming toward a ROI. The array is chosen so that a robust beamformer with high directivity may be designed toward any possible look direction in the ROI. As opposed to genetic algorithms and greedy-based approaches, our method can find the global optimum geometry via convex optimization methods. We show that the proposed method yields higher directivity than a ULA geometry and a dense differential microphone array (DMA) geometry.

This work was supported by the Pazy Research Foundation.

2. SIGNAL MODEL AND PROBLEM FORMULATION

Consider a system with M omnidirectional microphones placed nonuniformly across a linear aperture A. Assuming a source of interest in the far-field emitting a signal toward the array, the observed signal in the frequency domain is given by the vector

$$\begin{aligned}\mathbf{y}(\omega) &\triangleq [Y_1(\omega), Y_2(\omega), ..., Y_M(\omega)]^T \\ &= \mathbf{d}(\mathbf{x},\omega,\theta) S(\omega) + \mathbf{v}(\omega) \end{aligned} \quad (1)$$

where the superscript ^{T} is the transpose operator, $Y_m(\omega)$ is the signal captured by the m-th microphone, $S(\omega)$ is the propagated signal, $\mathbf{v}(\omega)$ is the additive noise vector, and

$$\mathbf{d}(\mathbf{x},\omega,\theta) = \left[e^{-\jmath\frac{\omega}{c}x_1\cos\theta}, e^{-\jmath\frac{\omega}{c}x_2\cos\theta}, ..., e^{-\jmath\frac{\omega}{c}x_M\cos\theta}\right]^T \quad (2)$$

is the array steering vector, where $\mathbf{x} \triangleq [x_1, x_2, ..., x_M]^T$ is the microphone position vector, θ is the signal incidence angle with respect to the endfire direction, $\omega = 2\pi f$ is the angular frequency, f is the temporal frequency, $\jmath$ is the imaginary unit, and c is the speed of sound, i.e., 340[m/s].

Utilizing all sensors in the array, we may design a beamforming filter

$$\mathbf{h}(\mathbf{x},\omega,\theta) \triangleq [H_1(\mathbf{x},\omega,\theta), H_2(\mathbf{x},\omega,\theta), ..., H_M(\mathbf{x},\omega,\theta)]^T \quad (3)$$

where $H_m(\mathbf{x},\omega,\theta)$ can be used to estimate the source signal of interest at angle θ by

$$\hat{S}(\omega) = \mathbf{h}^H(\mathbf{x},\omega,\theta)\,\mathbf{y}(\omega), \quad (4)$$

where the superscript ^{H} is the complex conjugate operator.

The beampattern is then defined by

$$\begin{aligned}\mathcal{B}\left[\mathbf{h}\left(\mathbf{x},\omega,\tilde{\theta}\right),\theta\right] &= \mathbf{d}^H(\mathbf{x},\omega,\theta)\,\mathbf{h}\left(\mathbf{x},\omega,\tilde{\theta}\right) \\ &= \sum_{m=1}^{M} H_m\left(\mathbf{x},\omega,\tilde{\theta}\right) e^{\jmath\frac{\omega}{c}x_m\cos\theta} \end{aligned} \quad (5)$$

which measures the response of the beamformer directed toward $\tilde{\theta}$ at an angle of arrival θ.

978-1-6654-6867-1/22/$31.00 ©2022 IEEE

A good measure of beamformer robustness in the presence of white noise is white noise gain (WNG):

$$\mathcal{W}\left[\mathbf{h}\left(\mathbf{x},\omega,\theta\right)\right] \triangleq \frac{\left|\mathbf{d}^{H}\left(\mathbf{x},\omega,\theta\right)\mathbf{h}\left(\mathbf{x},\omega,\theta\right)\right|^{2}}{\mathbf{h}^{H}\left(\mathbf{x},\omega,\theta\right)\mathbf{h}\left(\mathbf{x},\omega,\theta\right)}. \quad (6)$$

As the look direction amplification increases with respect to noise amplification, the WNG increases.

Another important measure is the directivity factor (DF), which measures beamformer performance in the presence of a diffuse noise field:

$$\mathcal{D}\left[\mathbf{h}\left(\mathbf{x},\omega,\theta\right)\right] \triangleq \frac{\left|\mathbf{d}^{H}\left(\mathbf{x},\omega,\theta\right)\mathbf{h}\left(\mathbf{x},\omega,\theta\right)\right|^{2}}{\mathbf{h}^{H}\left(\mathbf{x},\omega,\theta\right)\mathbf{\Gamma}\left(\mathbf{x},\omega\right)\mathbf{h}\left(\mathbf{x},\omega,\theta\right)} \quad (7)$$

where

$$\mathbf{\Gamma}_{i,j}\left(\mathbf{x},\omega\right) = \frac{\sin\left(\omega\left(x_i - x_j\right)/c\right)}{\omega\left(x_i - x_j\right)/c}, \quad 1 \le i,j \le M. \quad (8)$$

This narrowband measurement may also be extended to the broadband case. We define the broadband directivity index over frequencies $\omega_L \le \omega \le \omega_H$ by

$$\mathcal{DI}_{[\omega_L,\omega_H]}\left[\mathbf{h}\left(\mathbf{x},\omega,\theta\right)\right] \triangleq \frac{\int_{\omega_L}^{\omega_H}\left|\mathbf{d}^{H}\left(\mathbf{x},\omega,\theta\right)\mathbf{h}\left(\mathbf{x},\omega,\theta\right)\right|^{2}d\omega}{\int_{\omega_L}^{\omega_H}\mathbf{h}^{H}\left(\mathbf{x},\omega,\theta\right)\mathbf{\Gamma}\left(\mathbf{x},\omega\right)\mathbf{h}\left(\mathbf{x},\omega,\theta\right)d\omega}. \quad (9)$$

We also denote $\omega_L = 2\pi f_L$ and $\omega_H = 2\pi f_H$.

Our objective is to find the optimal array geometry $\mathbf{x}$, that maximizes the worst-case directivity index, as in (9), in a ROI around the endfire direction $|\theta| \le \theta_H$. Each beamformer, directed toward θ, must admit to the distortionless constraint, have sufficient WNG, and maintain a minimal distance between two microphones. This problem can be expressed mathematically as

$$\begin{aligned}\mathbf{x}^{*} = \arg\max_{\mathbf{x}} \quad & \min_{\theta\in\Theta}\mathcal{DI}_{[\omega_L,\omega_H]}\left[\mathbf{h}\left(\mathbf{x},\omega,\theta\right)\right] \\ \text{s.t.} \quad & \mathcal{B}\left[\mathbf{h}\left(\mathbf{x},\omega,\theta\right),\theta\right] = 1 \qquad \forall\theta\in\Theta,\forall\omega\in\Omega \\ & \mathcal{W}\left[\mathbf{h}\left(\mathbf{x},\omega,\theta\right)\right] \ge \delta \qquad \forall\theta\in\Theta,\forall\omega\in\Omega \\ & \left|x_i - x_j\right| \ge d_c \qquad \forall i,j\in[1,M], i\ne j \\ & 0 \le x_m \le A \qquad \forall m\in[1,M]\end{aligned} \quad (10)$$

where δ is the minimal WNG, d_c is the minimal distance between two adjacent microphones (half of microphone physical space), $\Omega = \{\omega : \omega_L \le \omega \le \omega_H\}$ marks the frequency range, $\Theta = \{\theta : |\theta| \le \theta_H\}$ marks the ROI, and $\mathbf{x}^{*}$ is the optimal array geometry.

3. OPTIMAL ARRAY DESIGN

To find $\mathbf{x}^{*}$, we formulate the problem as a convex one. First, we present the constraints, then the target function.

3.1. Constraints

We start by sampling our search space. Consider a grid of N possible microphone locations $[0 : \Delta x : A]$, where

$$\Delta x = \frac{A}{N-1}. \quad (11)$$

We define a selection vector optimization variable

$$\mathbf{s} = \left[S_1,...,S_{N-1},1\right]^{T} \quad (12)$$

which consists of binary values. Each element S_i is 1 if a microphone is placed at distance $(i-1)\Delta x$ with respect to the rightmost placement, and is 0 otherwise. Note that, without loss of generality, the leftmost coordinate is always occupied, i.e., $S_N = 1$. This is done to increase the search grid of the array effectively. To guarantee the existence of only M microphones, we should constrain $\mathbf{s}$ to $\mathcal{C}_1$:

$$\mathcal{C}_1\left[\mathbf{s}\right] : \mathbf{s}^{H}\mathbf{i}_N = M \quad (13)$$

where $\mathbf{i}_N$ is a column vector of length N consisting of ones.

To guarantee minimal distances, we must ensure that all adjacent selected placements will be separated by at least d_c. This means that there are restricted areas where no more than a single microphone can be present. All elements of S that correspond to such an area are summed and constrained to be no more than 1. Mathematically, this is described by $\mathcal{C}_2$:

$$\mathcal{C}_2\left[\mathbf{s}\right] : \mathbf{s}^{H}U \le \mathbf{i}_G^{T} \quad (14)$$

where $G = N - \lfloor\frac{d_c}{\Delta x}\rfloor$ is the number of restricted areas, U is a matrix of dimensions $N \times G$, whose i-th column is of the form

$$u_i = \left[\mathbf{0}_{i-1}^{T},\mathbf{i}_{N+1-G}^{T},\mathbf{0}_{G-i}^{T}\right]^{T}, \quad (15)$$

and $\mathbf{0}_i$ is a column vector consisting zeros of length i.

Now, in addition to the variable $\mathbf{s}$, we must take into account the coefficient variables. To this end, we denote by

$$\mathbf{h}_{\text{tot}}\left(\omega,\theta\right) = \left[H_{\text{tot},1}\left(\omega,\theta\right),H_{\text{tot},2}\left(\omega,\theta\right),...,H_{\text{tot},N}\left(\omega,\theta\right)\right]^{T} \quad (16)$$

a vector that corresponds to a beamformer directed toward θ that utilizes all N potential sensor placements. Sampling in frequency space and angle space, we consider several frequencies $[\omega_L : \Delta\omega : \omega_H]$ where

$$\Delta\omega = \frac{\omega_H - \omega_L}{Q-1}, \quad \omega_q = \omega_L + (q-1)\Delta\omega, \quad q\in[1,Q] \quad (17)$$

and several look directions $[0 : \Delta\theta : \theta_H]$ where

$$\Delta\theta - \frac{\theta_H}{P-1}, \quad \theta_p = (p-1)\Delta\theta, \quad p\in[1,P]. \quad (18)$$

Thus, we can sample the coefficients $\mathbf{h}_{\text{tot}}\left(\omega,\theta\right)$ on several values of ω and θ, overall involving $N\times Q\times P$ coefficient variables in our optimization. Note that only positive values of θ are taken into account due to the performance symmetry of linear arrays with respect to the endfire direction.

To admit to the distortionless constraint, the beampattern of any beamformer at any frequency toward the look direction should be 1. This is constrained by $\mathcal{C}_3$:

$$\mathcal{C}_3\left[\mathbf{h}_{\text{tot}}\left(\omega,\theta\right)\right] : \mathbf{d}_{\text{tot}}^{H}\left(\omega_q,\theta_p\right)\mathbf{h}_{\text{tot}}\left(\omega_q,\theta_p\right) = 1 \quad \forall p\in[1,P], \quad \forall q\in[1,Q], \quad (19)$$

where

$$\mathbf{d}_{\text{tot}}\left(\omega,\theta\right) = \left[1,e^{-\jmath\frac{\omega}{c}\Delta x\cos\theta},...,e^{-\jmath\frac{\omega}{c}A\cos\theta}\right]^{T}. \quad (20)$$

When the distortionless constraint is satisfied, it is sufficient to use $\mathcal{C}_4$ to maintain the desired WNG:

$$\mathcal{C}_4\left[\mathbf{h}_{\text{tot}}\left(\omega,\theta\right)\right] : \mathbf{h}_{\text{tot}}^{H}\left(\omega_q,\theta_p\right)\mathbf{h}_{\text{tot}}\left(\omega_q,\theta_p\right) \le \frac{1}{\delta} \quad \forall p\in[1,P], \quad \forall q\in[1,Q]. \quad (21)$$

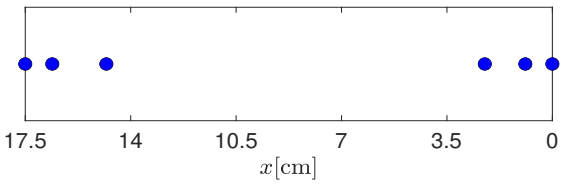

Fig. 1. *Optimal array geometry for* $M = 6$, $d_c = 0.5$ *cm*, $A = 17.5$ *cm*, $\theta_H = 30^\circ$, $f_L = 2$ *kHz*, $f_H = 6$ *kHz, and* $\delta = -10$ *dB*.

Finally, utilizing only M microphones in practice, the following must hold:

$$\mathcal{C}_5\left[\mathbf{s}, \mathbf{h}_{\text{tot}}\left(\omega,\theta\right)\right] : \left|H_{\text{tot},i}\left(\omega_q,\theta_p\right)\right|^2 \leq \frac{S_i}{\delta} \quad \forall i \in [1,N], \quad \forall p \in [1,P], \quad \forall q \in [1,Q]. \tag{22}$$

Essentially, if $S_i = 0$, then all beamformers will not utilize the i-th microphone placement. In practice, this means that no microphone is placed at $(i-1)\Delta x$. However, if $S_i = 1$, then there is indeed a microphone placed, and all beamformers may utilize that position. The factor $1/\delta$ provides an upper bound so that $\mathcal{C}_5$ is convex. As long as $\mathcal{C}_4$ is also maintained, this factor does not restrict the coefficients further.

3.2. Target Function

Notice that when the distortionless constraint is met, the numerator in (9) is constant:

$$\int_{\omega_L}^{\omega_H} \left|\mathbf{d}^H\left(\mathbf{x},\omega,\theta\right)\mathbf{h}\left(\mathbf{x},\omega,\theta\right)\right|^2 d\omega = \int_{\omega_L}^{\omega_H} \left|\mathcal{B}\left[\mathbf{h}\left(\mathbf{x},\omega,\theta\right),\theta\right]\right|^2 d\omega = \int_{\omega_L}^{\omega_H} d\omega = \omega_H - \omega_L. \tag{23}$$

Therefore, when maximizing the directivity index, we may focus on minimizing the denominator of (9). When approximating the integral to a discrete sum, using our optimization variables, we get

$$\int_{\omega_L}^{\omega_H} \mathbf{h}^H\left(\mathbf{x},\omega,\theta\right)\mathbf{\Gamma}\left(\mathbf{x},\omega\right)\mathbf{h}\left(\mathbf{x},\omega,\theta\right)d\omega \propto \sum_{q=1}^{Q} \mathbf{h}_{\text{tot}}^H\left(\omega_q,\theta\right)\mathbf{\Gamma}_{\text{tot}}\left(\omega_q\right)\mathbf{h}_{\text{tot}}\left(\omega_q,\theta\right), \tag{24}$$

where $\mathbf{\Gamma}_{\text{tot}}\left(\omega\right)$ is of dimensions $N \times N$ with elements

$$\mathbf{\Gamma}_{\text{tot},i,j}\left(\omega\right) = \frac{\sin\left[\omega\left(i-j\right)\Delta x/c\right]}{\omega\left(i-j\right)\Delta x/c}, \quad 1 \leq i,j \leq N. \tag{25}$$

To maximize the worst-case directivity index as in (10), the maximal value of (24) over $\theta \in \Theta$ should be minimized. Thus, we should find the minimum of

$$R\left[\mathbf{h}_{\text{tot}}\left(\omega,\theta\right)\right] = \max_{p\in[1,P]} \sum_{q=1}^{Q} \mathbf{h}_{\text{tot}}^H\left(\omega_q,\theta_p\right)\mathbf{\Gamma}_{\text{tot}}\left(\omega_q\right)\mathbf{h}_{\text{tot}}\left(\omega_q,\theta_p\right). \tag{26}$$

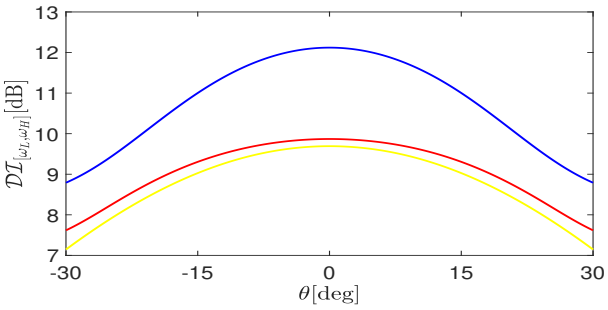

Fig. 2. *Directivity index as function of* θ *for the competing methods. The blue, red, and yellow lines mark the proposed, ULA, and dense geometries, respectively.* $M = 6$, $d_c = 0.5$ *cm*, $A = 17.5$ *cm*, $\theta_H = 30^\circ$, $f_L = 2$ *kHz*, $f_H = 6$ *kHz, and* $\delta = -10$ *dB*.

Notice that $R\left[\mathbf{h}_{\text{tot}}\left(\omega,\theta\right)\right]$ is a convex function, since it is the maximum of convex functions [25].

Since the target function and constraints are all convex, we can solve the mixed-integer convex optimization problem

$$\begin{aligned} \min_{\mathbf{s},\mathbf{h}_{\text{tot}}(\omega,\theta)} \quad & R\left[\mathbf{h}_{\text{tot}}\left(\omega,\theta\right)\right] \\ \text{s.t.} \quad & \mathcal{C}_1\left[\mathbf{s}\right], \mathcal{C}_2\left[\mathbf{s}\right], \mathcal{C}_3\left[\mathbf{h}_{\text{tot}}\left(\omega,\theta\right)\right], \\ & \mathcal{C}_4\left[\mathbf{h}_{\text{tot}}\left(\omega,\theta\right)\right], \mathcal{C}_5\left[\mathbf{s},\mathbf{h}_{\text{tot}}\left(\omega,\theta\right)\right]. \end{aligned} \tag{27}$$

The non-zero elements of the optimal binary vector $\mathbf{s}^*$ yield the optimal microphone locations $\mathbf{x}^*$. The non-zero elements of the optimal coefficients $\mathbf{h}_{\text{tot}}^*\left(\omega,\theta\right)$ yield the optimal coefficients $\mathbf{h}^*\left(\mathbf{x}^*,\omega,\theta\right)$.

4. COEFFICIENT POST-PROCESSING

Once $\mathbf{x}^*$ is found, the coefficients $\mathbf{h}^*\left(\mathbf{x}^*,\omega,\theta\right)$ are chosen so that the worst-case directivity index in the ROI is maximized. Thus, beamformers directed toward other directions in the ROI may not yield the best possible directivity. To circumvent this, given $\mathbf{x}^*$, a post-processing scheme is introduced.

The post-processed coefficients must have sufficient WNG and maximize the DF. Given the geometry $\mathbf{x}^*$, this can be done by finding the robust superdirective beamformer

$$\mathbf{h}_\epsilon\left(\mathbf{x}^*,\omega,\theta\right) = \frac{\mathbf{\Gamma}_\epsilon^{-1}\left(\mathbf{x}^*,\omega\right)\mathbf{d}\left(\mathbf{x}^*,\omega,\theta\right)}{\mathbf{d}^H\left(\mathbf{x}^*,\omega,\theta\right)\mathbf{\Gamma}_\epsilon^{-1}\left(\mathbf{x}^*,\omega\right)\mathbf{d}\left(\mathbf{x}^*,\omega,\theta\right)} \tag{28}$$

where

$$\mathbf{\Gamma}_\epsilon\left(\mathbf{x}^*,\omega\right) = \mathbf{\Gamma}\left(\mathbf{x}^*,\omega\right) + \epsilon\mathbf{I}_M, \tag{29}$$

$\mathbf{I}_M$ is the identity matrix of dimensions $M \times M$, and ϵ is a tradeoff parameter between WNG and DF.

We can decompose $\mathbf{\Gamma}\left(\mathbf{x}^*,\omega\right)$ as

$$\mathbf{\Gamma}\left(\mathbf{x}^*,\omega\right) = \mathbf{Q}\left(\mathbf{x}^*,\omega\right)\mathbf{\Lambda}\left(\mathbf{x}^*,\omega\right)\mathbf{Q}^T\left(\mathbf{x}^*,\omega\right) \tag{30}$$

where $\mathbf{\Lambda} = \text{diag}\left[\lambda_1,\lambda_2,...,\lambda_M\right]$ is the eigenvalue matrix such that $\lambda_1 \geq \lambda_2 \geq ... \geq \lambda_M$, and $\mathbf{Q}$ is the eigenvector matrix. As in [4], a robust superdirective beamformer that maintains sufficient WNG can be found for some ϵ in

$$0 \leq \epsilon \leq \frac{\lambda_1 - \sqrt{M/\delta}\lambda_M}{\sqrt{M/\delta} - 1}. \tag{31}$$

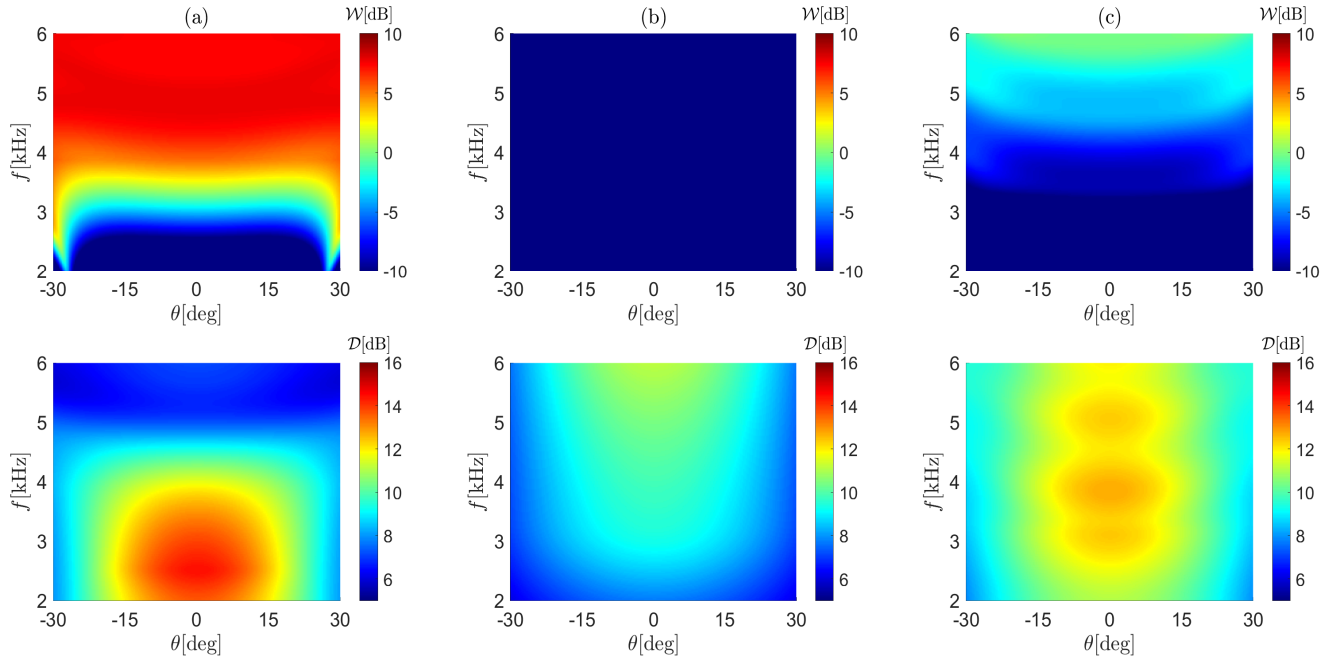

Fig. 3. *WNG and DF as function of f and θ for the competing methods: (a) ULA geometry, (b) dense geometry, and (c) proposed geometry. $M = 6$, $d_c = 0.5$ cm, $A = 17.5$ cm, $\theta_H = 30^\circ$, $f_L = 2$ kHz, $f_H = 6$ kHz, and $\delta = -10$ dB.*

Thus, for any ω and θ, we can run a bisection search on ϵ in this range to find the robust superdirective beamformer that yields the highest directivity yet has sufficient WNG. Subsequently, the beamformer is normalized so that the distortionless constraint is met.

5. SIMULATIONS

To solve the mixed-integer convex problem in (27), the MATLAB CVX toolbox [26] is used with the MOSEK [27] solver. We search for the optimal placement of $M = 6$ microphones on an aperture of length $A = 17.5$ cm where microphones are separated by at least $d_c = 0.5$ cm. Frequencies from $f_L = 2$ kHz to $f_H = 6$ kHz and look directions up to $\theta_H = 30^\circ$ are considered. Minimum WNG is set to $\delta = -10$ dB. Placements, frequencies, and look directions are sampled by $N = 40$, $Q = 15$, and $P = 15$, respectively. Our results are compared with a ULA geometry spread on all A, and the most dense feasible geometry (i.e., ULA with spacing d_c). The compared geometries also use M microphones. Theoretically, the dense geometry has an advantage in the endfire direction [1]. Coefficient post-processing, as described in Section 4 was applied to all geometries.

Figure 1 shows the optimal geometry $\mathbf{x}^*$. The resulting positions of the microphones are dense near the edges, and a large gap is present in the middle. The reasoning is that some microphones are placed close to each other to avoid low directivity due to spatial aliasing in high frequencies. On the other hand, some microphones are placed far from each other to maintain high spatial resolution for lower frequencies.

In Figure 2, the broadband directivity index as a function of look direction θ is shown for the competing methods. The proposed method has the highest minimum directivity index across $\theta \in \Theta$. Most importantly, superior performance is also achieved in any look direction by itself.

Figure 3 illustrates the WNG and DF as a function of frequency f and look direction θ for the competing methods. Using the ULA, a high directivity is achievable for low frequencies, yet the directivity deteriorates for high frequencies. This is due to spatial aliasing; the high WNG can no longer be exchanged for the sake of directivity. Considering the dense geometry, high directivity can be obtained for high frequencies, yet it is still comparatively low. This happens because the WNG is at its lowest possible value, a well-known problem associated with DMAs. The optimal geometry achieves high directivity across all frequencies, thereby maximizing the broadband directivity index.

6. CONCLUSIONS

We have presented an algorithm that finds the optimal microphone locations for broadband directivity in a ROI. Our method places some microphones closely to avoid spatial aliasing in high frequencies, and sets others further apart for spatial resolution in lower frequencies. We have shown that our design outperforms standard designs considering the worst-case look direction. Furthermore, excellent performance is achieved over all possible look directions as well. For simplicity, we have demonstrated our approach for a nonuniform linear geometry, but it can be extended to other geometries, including two and three-dimensional arrays.

7. REFERENCES

[1] J. Benesty, I. Cohen, and J. Chen, *Fundamentals of signal enhancement and array signal processing*, Wiley, 2018.

[2] J. Benesty, M. M. Sondhi, and Y. A. Huang, *Springer Handbook of Speech Processing*, Springer, 2008.

[3] M. Brandstein and D. Ward, *Microphone arrays: Signal processing techniques and applications*, Springer-Verlag, 2001.

[4] X. Chen, C. Pan, J. Chen, and J. Benesty, "Planar array geometry optimization for region sound acquisition," in *Proc. ICASSP*, 2021, pp. 756–760.

[5] K. Chen, X. Yun, Z. He, and C. Han, "Synthesis of sparse planar arrays using modified real genetic algorithm," *IEEE Transactions on Antennas and Propagation*, vol. 55, pp. 1067–1073, 2007.

[6] R. L. Haupt, "Thinned arrays using genetic algorithms," *IEEE Transactions on Antennas and Propagation*, vol. 42, pp. 993–999, 1994.

[7] F. L. Courtois, J. Thomas, F. Poisson, and J. Pascal, "Genetic optimisation of a plane array geometry for beamforming. application to source localisation in a high speed train," *Journal of Sound and Vibration*, vol. 371, pp. 78–93, 2016.

[8] J. Yu, F. Yu, and Y. Li, "Optimization of microphone array geometry with evolutionary algorithm," *Journal of Computers*, vol. 8, pp. 200–207, 2013.

[9] Z. Li, K. F. C. Yiub, and Z. Feng, "A hybrid descent method with genetic algorithm for microphone array placement design," *Applied Soft Computing*, vol. 13, pp. 1486–1490, 2013.

[10] A. Frank and I. Cohen, "Constant-beamwidth kronecker product beamforming with nonuniform planar arrays," *Frontiers in Signal Processing*, 2022.

[11] Y. Gershon, Y. Buchris, and I. Cohen, "Greedy sparse array design for optimal localization under spatially prioritized source distribution," in *Proc. ICASSP*, 2020, pp. 4607–4611.

[12] Y. Buchris, I. Cohen, J. Benesty, and A. Amar, "Joint sparse concentric array design for frequency and rotationally invariant beampattern," *IEEE/ACM Trans. Audio, Speech, Lang. Process*, vol. 28, pp. 1143–1158, 2020.

[13] Z. Zhong, M. Shakeel, K. Itoyama, K. Nishida, and K. Nakadai, "Assessment of a beamforming implementation developed for surface sound source separation," in *IEEE/SICE International Symposium on System Integration*, 2021, pp. 369–374.

[14] Z. Zhong, K. Itoyama, K. Nishida, and K. Nakadai, "Design and assessment of a scan-and-sum beamformer for surface sound source separation," in *IEEE/SICE International Symposium on System Integration*, 2020, pp. 808–813.

[15] M. Taseska and E. A. P. Habets, "Spotforming: spatial filtering with distributed arrays for position-selective sound acquisition," *IEEE/ACM Trans. Audio, Speech, Lang. Process*, vol. 24, pp. 1291–1304, 2016.

[16] J. Martinez, N. Gaubitch, and W. B. Kleijn, "A robust region-based near-field beamformer," in *Proc. ICASSP*, 2015, pp. 2494–2498.

[17] M. Taseska and E. A. P. Habets, "Spotforming using distributed microphone arrays," in *Proc. WASPAA*, 2013, pp. 1–4.

[18] H. Jo, Y. Park, and Y. S. Park, "A sound telescope: a control of zone of interest," in *Proc. ICA*, 2010, pp. 1–5.

[19] A. Davis, S. Y. Low, S. Nordholm, and N. Grbic, "A subband space constrained beamformer incorporating voice activity detection [speech enhancement applications]," in *Proc. ICASSP*, 2005, pp. 65–68.

[20] J. Chen, L. Shue, H. Sun, and K. Phua, "An adaptive microphone array with local acoustic sensitivity," in *IEEE International conference on multimedia and expo*, 2005, pp. 1–4.

[21] N. Grbić and S. Nordholm, "Soft constrained subband beamforming for hands-free speech enhancement," in *Proc. ICASSP*, 2002, pp. 885–888.

[22] A. Kleiman, I. Cohen, and B. Berdugo, "Constant-beamwidth beamforming with concentric ring arrays," *Sensors, 7253*, pp. 1–19, 2021.

[23] T. Long, I. Cohen, B. Berdugo, Y. Yang, and J. Chen, "Window-based constant beamwidth beamformer," *Special Issue of Sensors on Speech, Acoustics, Audio Signal Processing and Applications in Sensors*, vol. 19, pp. 1–20, 2019.

[24] O. Rosen, I. Cohen, and D. Malah, "FIR-based symmetrical acoustic beamformer with a constant beamwidth," *Signal Processing*, vol. 130, pp. 365–376, 2017.

[25] S. Boyd and L. Vandenberghe, *Convex Optimization*, Cambridge university press, 2004.

[26] M. Grant and S. Boyd, "CVX: Matlab software for disciplined convex programming," 2014.

[27] MOSEK ApS, "The MOSEK optimization toolbox for Matlab 9.1," 2019.